Earthquake Forces on the Stability of the Meninting Diversion Tunnel Design Based on Current Seismic Conditions of Lombok Island

Didi S. Agustawijaya[1], Rian M. Taruna[2], and Ausa R. Agustawijaya[3]

[1]Geo-Engineering Research Group, Department of Civil Engineering, University of Mataram, Mataram 83125, Indonesia
[2]Indonesian Agency for Meteorology, Climatology and Geophysics (BMKG), Mataram, Indonesia
[3]Department of Geomatics Engineering, ITS, Surabaya, Indonesia

Corresponding author: didiagustawijaya@unram.ac.id
Manuscript received: April, 25, 2020; revised: February, 2, 2020;
approved: April, 5, 2021; available online: January, 28, 2022

Abstract - A series of earthquakes in 2018 have ruined thousands of buildings, and affected the stability of many infrastructures in Lombok Island. The Meninting dam, located at just a 20 km distance from the epicentre of the 5th August earthquake, is one of the many infrastructures being constructed in the island. Unfortunately, stability problems might arise to the dam, in particular to its diversion-spillway tunnel, since the tunnel was designed by using the Indonesian Standards SNI 1726:2012 for the estimation of earthquake forces into the design. After the earthquake events in 2018, seismic conditions of Lombok Island changed, resulted in changing seismic parameters. Seismic forces might shear off the friable weak volcanic rocks around the tunnel, and then consequently, the residual strength of the rocks had to stand the tunnel construction, so its factor of safety reduced. Thus, the tunnel required some stability improvements by adding more support instalments, including grouting and rock bolting. This is important for the tunnel to face probable similar severe earthquakes in the future.

Keywords: Lombok earthquake, Meninting tunnel, seismic force, volcanic rock, residual strength, stability

INTRODUCTION

Background

A series of shallow earthquakes occurring during July to September 2018 have ruined thousands of houses and buildings in Lombok Island (Irsyam *et al.*, 2018; Pramono, 2018; Agustawijaya *et al.*, 2019). Unfortunately, Lombok Island is located in the Nusa Tenggara region, which is one of the most active seismic parts in Indonesia. As can be seen in Figure 1 for the particular tectonic setting of eastern Indonesia, the Australian Continental Plate subducts beneath the Eurasian Plate (Hamil-

ton, 1979); while the Pacific Plate that compresses the Sunda-Banda Arc moves westward (Katili, 1989; Bock *et al.*, 2003; Verstappen, 2010). This tectonic setting, therefore, exposes vulnerability to seismic hazards for Lombok Island (Koulali *et al.*, 2016; Griffin and Davies, 2018), where seismic forces may trigger the activity of the Flores Fault just located along the north coast of Nusa Tenggara (Pranantyo and Cummins, 2019), as occurred in 2018 (Agustawijaya *et al.*, 2020a).

One of many projects being constructed in Lombok Island is the Meninting dam. The dam had two tunnels: intake and diversion-spillway.
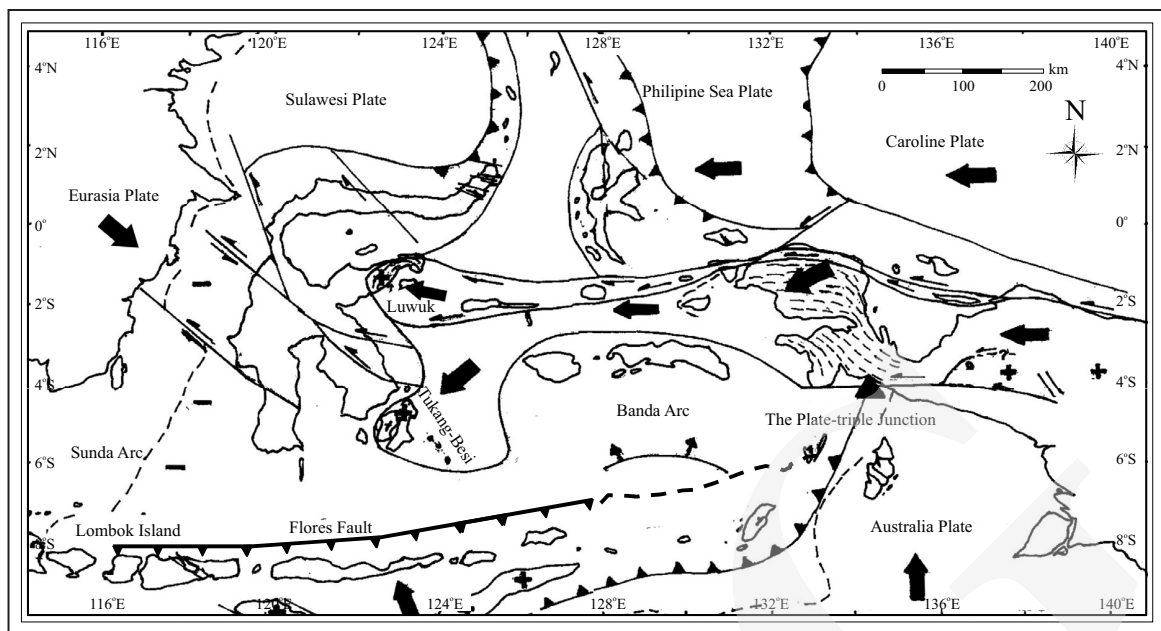
Figure 1. Tectonic patterns and plate movements of eastern Indonesia, where Lombok Island just located on the edge between the Sunda Arc and the Banda Arc (modified from Katili, 1989; Verstappen, 2010; Koulali *et al*., 2016).

Unfortunately, the tunnels were designed using the old Indonesian standards SNI 1726:2012 (BSNI, 2012) for calculating their stability under earthquakes. Although the standards have been replaced with the SNI 1726:2019 (BSNI, 2019), the new standards are still using earthquake data before the 2018 events, in which the data were up to 2016.

Agustawijaya *et al*. (2020b) had proposed updated seismic data for Nusa Tenggara Region. The proposed data show increases in seismic parameter values, which indicate particularly higher seismic hazard vulnerability to Lombok Island.

Considering changes in seismic parameters and uncertainty factors in designing the tunnels, an evaluation on stability should be an important subject to current seismic parameters, which are different from those when the tunnels were designed in 2017 (BWS, 2017).

Seismic Intensity and Hazard

A series of earthquakes in 2018 had been devastating the Lombok Island and ruined thousands of building. These earthquakes were triggered by the Flores Fault at the backarc basin of Lombok Island (Pranantyo and Cummins, 2019). The intensity of the events, particularly in 5th August 2018, was from MMI III to IX (Taruna, 2019). The Meninting dam location had MMI VII (Figure 2), and it was reported that people were hard to stand up, vehicle were shacked, most walls of building felt down, and many buildings collapsed (BMKG, 2018). This could mean that the site had some collapsed area in terms of rock failures and landslides (Irsyam *et al*., 2018).

Proposed probabilistic seismic hazard analysis (PSHA) by Agustawijaya *et al.* (2020b) showed that seismic sources of Lombok Island were developed by three sources: subduction, background, and shallow fault. This probabilistic seismic hazard analysis resulted in higher seismic parameter values compared to those suggested by Irsyam *et al.* (2017). The Gutenberg-Richter *a*- and *b*-parameters, peak ground acceleration values, as well as other spectral hazard values were higher than those estimated in 2017. These values indicate that Lombok and surrounding islands are exposed to a higher seismic hazard than that was predicted before the earthquake events in 2018. Based on this analysis, after the events in 2018, seismic hazard parameters increased about 6% than those estimated in 2017 (Irsyam *et al.*, 2017).
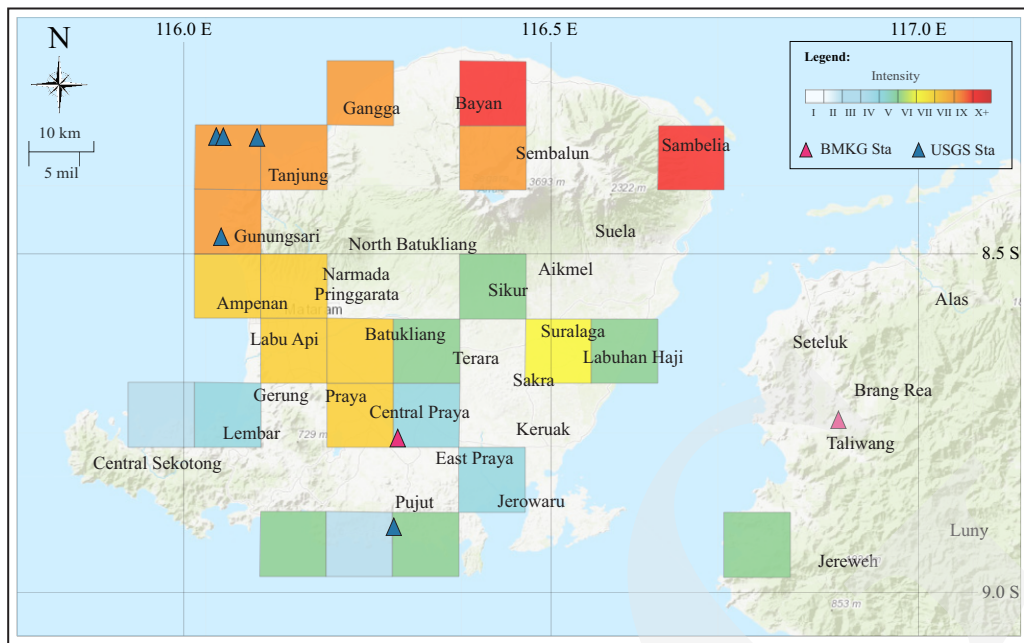
Figure 2. The intensity of the earthquake event in 5th August 2018 around Lombok Island, the location of Meninting dam included into MMI VII (Modified from USGS, 2018).

The probabilistic analysis with an applied exceedance probability of 2% in fifty years, resulted in the PGA values of bed rocks were 0.6 - 0.7 g for mostly Lombok, and the highest PGA value was 0.75 g for Bayan located at the North Lombok District, where the epicentre of the 5th August 2018 event was located. The short seismic spectrum Ss was in the range of 1.0 - 1.2 g, and the north part of Lombok Island had the highest value of 1.2 g. The long seismic spectrum S_1 was in the range of 0.25 - 0.6 g.

Tunnel Design

The Meninting dam was designed to have two tunnels: intake, and diversion-spillway. The intake tunnel had a dimension of 4.6 x 4.6 x 457.15 m, located at the left flank of the dam. Two tunnel shapes were applied depending on the position along the tunnel: the square shape for inlet through intake gate; while the curved shoe-shape for the rest of the intake tunnel of 330.3 m in length. The elevation of the tunnel base was at +167 m above the mean sea level (MSL), and the top surface elevation of this tunnel was at +202.0 m above the MSL.

The diversion-spillway tunnel was designed to be of two types: Type 1 and Type 2 (Figure 3).

The type 1was a diversion tunnel, which had a dimension of 5.20 x 5.20 x 129.5 m. The type 2 was a spillway tunnel, which had a dimension of 9.40 x 9.40 x 252.5 m. Then, the type 1 would be connected with a 10 m transitional tunnel to the type 2 to become a diversion-spillway tunnel. A spillway inlet would be above the tunnel, a connecting shaft of a 9.18 m diameter would then be inclined 22⁰ from the spillway inlet to the base of the diversion-spillway tunnel. The position of this tunnel was planned at the right flank of the dam. The elevation of the tunnel base would be at +147.8 m above the MSL, while the top surface of the tunnel would be at +211.9 m above the MSL.

The diversion-spillway shoe-shaped tunnel, which is similar to the typical tunnel of the Cirata mega project reported by Harjomuljadi (2010), was planned to have full support systems, including wiremesh with a 0.15 m thickness of shotcrete, steel H-beams installed with a spacing of 1 m, a concrete lining of 0.6 m thickness, consolidation and curtain grouts. Then, far field stresses, P on vertical and kP on horizontal directions,were estimated on each part of the tunnel: A, B, C, D, E; and additional stresses of earthquake were estimated working on perpendicular to tunnel axis (Figure 4).
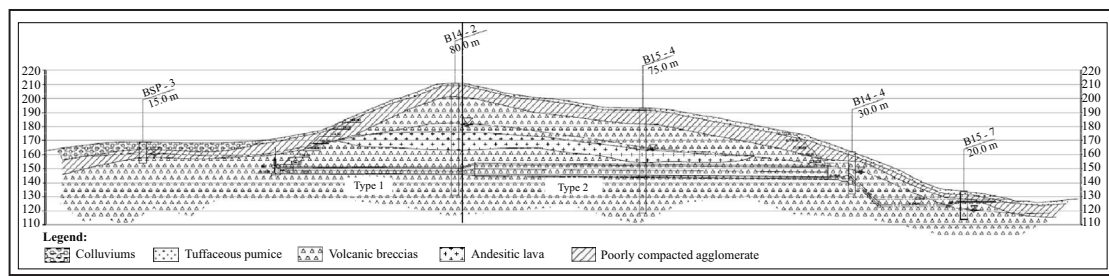
Figure 3. Long section of the Meninting tunnel of Type1 (diversion tunnel) and Type 2 (spillway tunnel), excavated into volcanic breccia rocks. The diversion tunnel will be connected with the spillway tunnel through transitional connecting part to become a diversion-spillway tunnel (modified from BWS, 2017).
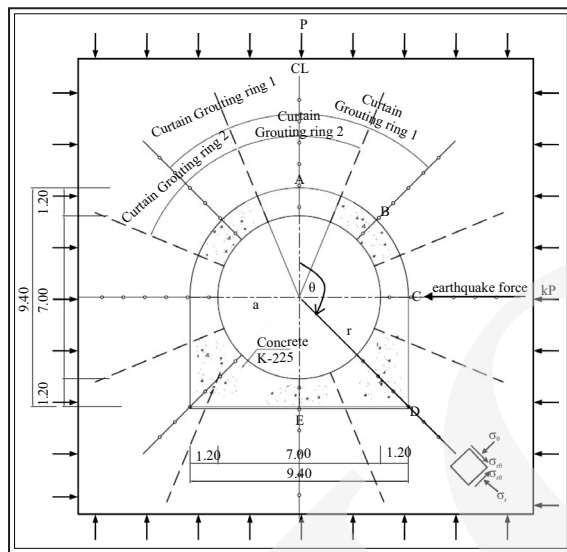

Figure 4. Type 2 of diversion tunnel with stresses working around tunnel: Crown A, Crown B, Wall C, Base D,and Base E are parts of tunnel being analyzed. Earthquake forces are horizontally working perpendicular to the tunnel axis, where a is radius and r is a point distance of estimations (tunnel design modified from BWS, 2017).

Geological Setting

Based on the geological map of Lombok Island (Andi Mangga *et al.*, 1994), the island comprises Tertiary (Early Miocene) until Holocene sedimentary rocks and intrusive andesitic igneous rocks. The oldest rock formation is the Pengulung Formation of Late Oligocene-Early Miocene sedimentary rocks, overlain by the Kawangan Formation of Middle Miocene sandstone. Both formations are located in the south where intrusive igneous rocks of Middle Miocene can also be found. The Ekas Formation of Late Miocene limestone overlaid the Pengulung and Kawangan Formations. In the north, young volcanic rocks dominate the geology of the is-

land, including the Kalipalung, Kalibabak, and Lekopiko Formations.

The location of the Meninting dam is at Dasan Gria, where the last three rock formations covered the area. These sedimentary rock materials contained volcanic breccias, lava, and poor compacted volcanic rock materials of agglomerates and colluviums. Most rock materials were from erupted rock materials of the RinjaniVolcano (Lavigne *et al.*, 2013).

As can be seen in Figure 3, based on the drilling holes of B14-2 and B15-4, rocks at the Meninting tunnel contained volcanic breccias on the base, with lava, agglomerates, and colluviums on the top of the tunnel (BWS, 2017).

Geological structures seem to be invisibly significant within the area, since thick sedimentary rocks covered the area. There were no physical features of faults within the area. But, when considering alignments at the south part of the island, general geological structures within the island might follow the model of Harding and Lowell (1979), such that the geological structure seems to develop on a basement sinistral strike-slip fault as the main structure in the direction of NW - SE, then minor shear strike-slip faults developing in the direction of SW - NE (Agustawijaya *et al.*, 2018). From this structural pattern, a direction of main forces working at Lombok Island can be drawn on N 171^{0}E - N 351^{0}E, and N 22 ^{0}E - N 202 ^{0}E. The NE - SW could be of the main major force direction working within the island, and it is in line with the regional tectonic pattern of the Sunda Arc (Katili, 1989); it might also be in a similar pattern with that of Java Island (Agustawijaya *et al.*, 2017).

METHODS

The Meninting dam and its tunnels have already been under construction since 2019 after a long delay due to the Lombok Earthquake 2018. The tunnel construction followed the New Austrian Tunnelling Method (NATM) (Harjomuljadi, 2010). The support systems of the tunnels utilized the geomechanic classification by Bieniawski (1989), in which the geological data inputs were based on the suggested methods by the International Society for Rock Mechanics (1981).

For the current stability analyses in this paper, the estimations of rock mass strength followed two criteria: the nonlinear Hoek-Brown (HB) (Hoek and Brown, 1994) and linear Mohr-Coulomb (Labuz and Zang, 2012). The HB was initially for jointed rock materials, and then used for rock mass, as follows (Hoek *et al.*, 2002):

$$\sigma_1 = \sigma_3 + \sigma_{ci}\left(m_b\,\frac{\sigma_3}{\sigma_{ci}}+s\right)^a \quad \text{..........................} (1)$$

According to Equation 1, the strength of rock masses will depend on parameters m_b, s and a, which can be obtained from the rock mass rating (RMR) proposed by Bieniawski (1989).

For weak granular rock masses, however, the linear Mohr-Coulomb might be modified by applying rock mass parameter R and M, as follows (Agustawijaya, 2018):

$$\sigma_1 = R\sigma_{ci} + M\sigma_3 \quad \text{...} (2)$$

where:
R is ratio of uniaxial compressive strength of rock mass and intact rock (σ_{cm}/σ_{ci}),
$M = \dfrac{1 + \sin\phi}{1 - \sin\phi}$, and
φ is friction angle.

Based on Equation 2, the rock mass strength will linearly depend on rock mass properties and confining stress σ_3.

Many uncertainties are involved in estimating rock mass strength, brought by the nature of rock materials, testing condition, and design application (Kulhawy *et al.*, 2001; Prakoso and Kulhawy, 2011; Serra and Miranda, 2013). For a seismic area, additional uncertainties will be from earthquake forces. When earthquake forces work on rock, the rock is under dynamic shear conditions. Then, the shear strength of rock depends on coefficient of friction and normal force of two conditions, *i.e.* static and dynamic (Brady and Brown, 1993). In these conditions, static stresses develop until the acceleration of earthquake forces gets the peak (Equation 3), and then the dynamic shear strength (Equation 4) will have a stress drop up to 10% from the static shear strength.

$$\tau_s = \mu_s\sigma_n \quad \text{...} (3)$$

$$\tau_d = \mu_d\sigma_n \quad \text{...} (4)$$

τ_s = static shear strength
μ_s = coefficient of static friction
σ_n = normal force
τ_d = dynamic shear strength
μ_d = coefficient of dynamic friction

Then, the estimation of stresses around the tunnel followed the Kirsch solutions (Hoek and Brown, 1994). Within these estimations (Equation 5), the far field stresses are P in the vertical direction, and kP in the horizontal direction. Then, stresses at a point (r, θ) around the tunnel will be calculated as radial (σ_r), tangential (σ_θ), and shear stresses ($\sigma_{r\theta}$), where θ is the angle between the vertical and r is line from the axis point, as in Figure 4 (Hoek and Brown, 1994):

$$\sigma_r = 0.5P\left[\left(1+k\right)\left(1-\frac{a^2}{r^2}\right)+\left(1-k\right)\left(1+\frac{3a^4}{r^4}-\frac{4a^2}{r^2}\right)\cos 2\theta\right]$$

$$\sigma_r = 0.5P\left[\left(1+k\right)\left(1+\frac{a^2}{r^2}\right)-\left(1-k\right)\left(1+\frac{3a^4}{r^4}\right)\cos 2\theta\right]$$

$$\sigma_{r\theta} = 0.5P\left[-\left(1-k\right)\left(1-\frac{3a^4}{r^4}+\frac{2a^2}{r^2}\right)\sin 2\theta\right] \cdots (5)$$

Seismic parameters applied for the tunnel design were based on the SNI 1726:2012(BSNI,

2012), which has been replaced with the SNI 1726:2019 (BSNI, 2019). However, data used in the standards were those proposed by Irsyam *et al.* (2017), which were before the events in 2018. Updated seismic parameters based on data of up to 2018 have been proposed by Agustawijaya *et al.* (2020b). Although, for seismic force estimations, the procedures still followed the SNI 1726:2019, and therefore, shear forces on a horizontal direction perpendicular to the tunnel axis are following Equation 6:

$$V = \frac{S_{Ds} \times I_e}{R} \times W \quad ....\ (6)$$

V   = shear force/earthquake force
S_{DS} = short spectrum acceleration at 0.2 second
Ie   = earthquake factor
R   = reduction factor
W   = weight

RESULTS

Rock Mass Strength Around Tunnel

The Meninting diversion-spillway tunnel was mainly excavated into volcanic breccias, although on the top of the tunnel, rocks consisted of lava, agglomerates, and colluviums. The RMR should be different for each rock type, and of course, other rock material parameters should also be different, such as cohesion, friction, and unit weight. As the tunnel Type 2 contained volcanic breccias, the rock mass quality index of RQD was 65% in average. This massive rock mass has been slightly to medium weathered, so it had a permeability coefficient (k) during drilling of 5×10^{-5} cm/second. Then, laboratory tests for uniaxial compressive strength of rock material show a low σ_{ci} of 5.9 MPa for typical volcanic breccias taken from the borehole B15-4 (BWS, 2017).These all rock parameters resulted in an RMR of 40. According to Hoek and Brown (1994), this poor rock mass quality would have a stand up time for the tunnel up to one week without any support system. The RMR of 40, m_i of 19 and confining pressures of

0.06 MPa were, therefore, used for estimations of rock mass strength (Equation 1).

However, as the tunnel is on the surface, confining pressure should be limited. The MMC parameters for the Equation 2 were a friction angle of 35^0 and cohesion of 0.10 MPa, respectively. Estimations for rock mass parameters of σ_{cm} and M for volcanic breccias followed Agustawijaya (2019). Therefore, rock mass strength calculations were given for each part of the tunnel according to Figure 4, and the results can be seen in Table 1.

Equation 1 provided low σ_1 values from 0.31 to 0.41 MPa depending on the rock position on the tunnel. These low σ_1 values were very much influenced by low confining pressures of 0.06 MPa. Also, a RMR of 40 did not really increase the rock mass strength, as it should be (Priest, 1993). However, using Equation 2, the σ_1 values were in the range of 0.56 - 0.65 MPa, which are higher than those of Equation 1. Although, σ_{cm} was low of 0.09 MPa, obtained from low σ_{ci} (Agustawijaya *et al.*, 2004; Agustawijaya, 2007), the strength was really not sensitive to confining pressure. The strength depended on frictional characteristic of the rocks, *i.e.* friction angle and cohesion.

Stresses Around Tunnel

Following the Kirsch solutions for stresses around the tunnel, each part of the tunnel had a different stress concentration working on each part. On the boundary when the radius a equals the distance of the point estimated r, the radial stress σ_r and the shear stress $\sigma_{r\theta}$ were zero, so the only tangential stress σ_θ had a nonzero value. When r = a+1 m, stress values on each part of the tunnel can be seen in Table 2.

The tangential stresses worked significantly on the Crown B, Wall C, and Base D; shear stress concentrations should be on the Crown B and Base D; while, the Crown A should be tensioned, and some heave might occur on the Base E.

Earthquake Stresses

Procedures given by the SNI 1726:2019 (BSNI, 2019) were followed to estimate earth-

Table 1. Results of The Rock Mass Strength of The Mininting Tunnel Type 2

Parameter	Crown A	Crown B	Wall C	Base D	Base E
Rock	Breccia	Breccia	Breccia	Breccia	Breccia
Unit weight, γ (MN/m³)	0.021	0.021	0.021	0.021	0.021
Depth of axis, H (m)	26.6	26.6	26.6	26.6	26.6
σ_{ci}, (MPa)	5.9	5.9	5.9	5.9	5.9
σ_3, (MPa)	0.06	0.05	0.06	0.07	0.07
Friction angle, φ^0	35	35	35	35	35
Cohesion, c (MPa)	0.10	0.10	0.10	0.10	0.10
M	3.69	3.69	3.69	3.69	3.69
σ_{cm} (MPa)	0.09	0.09	0.09	0.09	0.09
m_i	19	19	19	19	19
RMR	40	40	40	40	40
σ_1 (1), (MPa)	0.36	0.32	0.36	0.41	0.39
σ_1 (2), (MPa)	0.59	0.56	0.59	0.65	0.63

Table 2. Stresses Working on Each Part of The Tunnel for r = a+1 m

Stress (MPa)	Crown A	Crown B	Wall C	Base D	Base E
σ_r	0.01	0.08	0.18	0.07	0.01
σ_θ	-0.09	0.22	0.63	0.29	-0.09
$\sigma_{r\theta}$	0.00	-0.20	0.00	0.20	0.00

quake forces for the Meninting diversion-spillway tunnel design, although, seismic parameters proposed by Agustawijaya *et al.* (2020b) were adopted for these calculations. Data of the SNI 1726:2019 and SNI 1726:2012 were, then, used for comparison. All seismic parameters can be seen in Table 3.

Earthquake forces working on the tunnel were considered to be horizontally perpendicular to the tunnel axis, and then the influence on the tunnel depended on the position on the tunnel. The earthquake stresses (Equation 6) on the peak Crown A and Base E were minimum; otherwise, on the Wall C were maximum of 0.34 MN/m² using current proposed seismic parameters (Table 4). This value increased by 26% from the value estimated using seismic parameters of the SNI 1726:2012, and by 18% from the value estimated using seismic parameters of the SNI 1726:2019.

Then, the earthquake stresses increased radial and tangential stresses working on the Crown B, Wall C, and Base D (Table 5). Again, the Wall C was under higher radial and tangential stresses, such tangential stresses were up to 1.01 MPa. This value increased 10% from designed value in 2017. However, tangential stresses $\sigma_{r\theta}$ decreased as the distance r increased. This can be seen in Figure 5, the stress was less significant to influence the

Wall C when the ratio r/a >1.5. Thus, the boundary of the Wall C would have more severe ruptures than that along the horizontal distance r.

Support Systems and Stability

The stability of the tunnel was described in terms of a factor of safety of each part of the tunnel. The factor of safety (FoS) of the tunnel after excavation and under the influence of earthquakes was calculated in terms of a ratio between rock mass strength and forces working around the tunnel subject to Kirsch formulations (Hoek and Brown, 1994).

The FoS values were estimated from the rock mass strength estimated from Equations 1 and 2 against stresses working on each part of the tunnel, particularly on the Crown B, Wall C, and Base D where stresses under the influence of earthquakes were concentrated. Under the influence of earthquakes, the stability of the tunnel without any support system reduced significantly down to 69%. The most deformed part of the tunnel was the Wall C, as earthquake forces were horizontally most working on the part.

The current seismic parameters increased the influence of earthquake forces by 5% on the stability of the tunnel from those estimated using the seismic parameters of the SNI 1726:2012 when

Table 3. Seismic Parameter for Estimating Earthquake Forces

Parameter	Proposed[1]	SNI 2019[2]	SNI 2012[3]
PGA (g)	0.65	0.50	0.43
S_{DS} (g)	1.08	0.90	0.80
S_{D1} (g)	0.65	0.40	0.40
F_A	1.0	1.00	1.00
F_V	1.5	1.50	1.50
$S_M = S_{DS} * F_A$ (g)	1.08	0.90	0.80
$S_{M1} = S_{D1} * F_V$ (g)	0.98	0.60	0.59
$S_{DS} = 2/3 * S_{MS}$ (g)	0.72	0.60	0.53
$S_{D1} = 2/3 * S_{M1}$ (g)	0.65	0.40	0.40
$T_0 = 0.2 * (S_{D1}/S_{DS})$ (sec)	0.18	0.13	0.15
$T_S = (S_{D1}/S_{DS})$ (sec)	0.9	0.67	0.74
Ie	1.25	1.25	1.25
R	1.2	1.2	1.2

PGA	=	peak ground acceleration	T = period of shaking
S_{DS}	=	short spectrum acceleration at 0.2 second	Ie = earthquake factor
S_{D1}	=	long spectrum acceleration at 1 second	R = reduction factor
F_A	=	coefficient of acceleration	[1]Agustawijaya *et al.* (2020b)
F_V	=	coefficient of velocity	[2]SNI 1726:2019 (BSNI, 2019)

Table 4. Earthquake Forces Working on Each Part of The Tunnel Based Current Proposed Seismic Parameters Compared with Those of 2019 and 2012

Tunnel Part	Earthquake Force V (MN/m²)		
	Proposed[1]	SNI 2019[2]	SNI 2012[3]
Crown A	0.00	0.00	0.00
Crown B	0.24	0.20	0.18
Wall C	0.34	0.28	0.25
Base D	0.24	0.20	0.18
Base E	0.00	0.00	0.00

the tunnel was design. The increase from the SNI 1726:2012 to the SNI 1726:2019 was only 1% in terms of the influence of seismic parameters on the stability of the tunnel.

According to Hoek and Brown (1994), the RMR of 40 provided stand up time for the tunnel up to one week prior to the installation of tunnel supports. If the FoS of <1.0 was considered, the estimated stand up time would be too long; and it would shorten, probably down to be twenty-five minutes when earthquake events were considered. Thus, supports should be immediately installed. As the tunnel construction applied the flexible

NATM (De Farias *et al.*, 2004), so all support systems were consequently installed as primary and secondary supports (Harjomuljadi, 2010).

When all tunnel supports were installed, including wire meshed shotcrete, H-steel beams, concrete lining of 0.6 m thickness and curtain and consolidation grouting, the tunnel would had a total additional strength of 10.23 MPa. This increased the strength of rock masses around the tunnel, particularly under influences of earth-
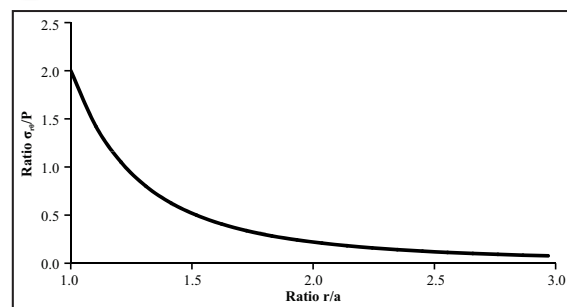
Figure 5. Variation in tangential stresses ($\sigma_{r\theta}$) on the Wall C according to ratio r/a.

Table 5. Radial (σ_r) and Tangential ($\sigma_{r\theta}$) Stresses after Earthquakes on Particular Parts of The Tunnel. Comparison between Estimations from Current Proposed, SNI 2019 and SNI 2012 Seismic Parameters

Tunnel Part	Stresses (MN/m²)					
	Proposed[1]		SNI 2019[2]		SNI 2012[3]	
	σ_r	$\sigma_{r\theta}$	σ_r	$\sigma_{r\theta}$	σ_r	$\sigma_{r\theta}$
Crown B	0.14	0.39	0.13	0.37	0.13	0.36
Wall C	0.29	1.01	0.27	0.95	0.26	0.91
Base D	0.11	0.42	0.10	0.40	0.10	0.39

[1]Agustawijaya *et al.* (2020b); [2]SNI 1726:2019 (BSNI, 2019); [3]SNI 1726:2012 (BSNI, 2012)

quake stresses working as shear stresses on the construction.

Unfortunately, the HB (Equation 1) still provided low FoS values of below 1.5 on these parts. However, the FoS estimated from the MMC (Equation 2) seemed to provide more engineering sound in terms of stability, as it provided FoS values of higher than 4.5 on the same parts of the tunnel (Table 6).

Table 6. Factor of Safety on Each Part of The Tunnel after The Completion of Support System Installations with Earthquakes Forces on The Directions of σ_r and σ_θ

Tunnel Part	Proposed[1]			
	HB/σ_r	HB/$\sigma_{r\theta}$	MMC/σ_r	MMC/ $\sigma_{r\theta}$
Crown B	3.65	1.32	32.60	11.79
Wall C	1.93	0.56	15.69	4.54
Base D	6.01	1.52	43.62	11.07

[1]Agustawijaya *et al.* (2020b)

Tunnel Part	SNI 2019[2]			
	HB/σ_r	HB/$\sigma_{r\theta}$	MMC/σ_r	MMC/ $\sigma_{r\theta}$
Crown B	3.84	1.39	34.29	12.40
Wall C	2.06	0.60	16.73	4.84
Base D	6.32	1.60	45.88	11.65

[2]SNI 1726:2019 (BSNI, 2019)

Tunnel Part	SNI 2012[3]			
	HB/σ_r	HB/$\sigma_{r\theta}$	MMC/σ_r	MMC/ $\sigma_{r\theta}$
Crown B	3.95	1.43	35.31	12.77
Wall C	2.14	0.62	17.37	5.03
Base D	6.51	1.65	47.25	12.00

[3]SNI 1726:2012 (BSNI, 2012)

DISCUSSION

Since a number of uncertainties involved in designing a tunnel, rock properties, size, and confinement have contributed into the strength of the rock mass of the Meninting tunnel. Rock properties and size might be represented by the RMR in this strength calculation. In addition to these, the estimated strength seems to increase when the confinement increases. The role of confining pressures seems to be significant when using the nonlinear equation (Agustawijaya, 2019).

As suggested by Eberhardt (2012), the nonlinear HB equation is dependent on the confinement, in which the criterion is controlled by the major and minor principal stresses. However, as the Meninting tunnel was excavated into weak

rocks at shallow depths, the σ_{ci} seemed to play a dominant role in estimating the strength of soft rock masses, similar to that of the Mila tunnel (Agustawijaya, 2019).

In terms of strength reduction, the σ_{cm} obtained from the measurement of cohesion and friction angle seems to provide more reliable results in the estimation (Al-Awad, 2012), particularly when the failure behaviour of the rock relies on shear strength of the rock. However, a σ_{cm} of 0.09 MN/m^2 provided a low rock mass strength, as well as a RMR of 40 resulted in a low rock mass strength using the nonlinear Hoek-Brown criterion. Although volcanic breccias around the tunnel do not show any significant structural features, a value of 40 was still too low to increase the rock mass strength. As suggested by Priest (1993), a rock mass that have an RMR of <63 would be categorized into soft rock masses, otherwise, it would increase the FoS up to 50%.

Under normal conditions, the instability of shallow tunnels in weak rocks may not be only caused by rock properties, but more important also by lack of confinement causing ground subsidence due to gravity loads. When the ratio of $(3\sigma_v - \sigma_3)/\sigma_{ci}$ is higher than 0.8, the tunnel will be very hard to support (Martin *et al.*, 1999). For the case of the Meninting tunnel, the ratio was 0.08. In addition to the ratio, Martin *et al.* (2003) suggested that the plastic yield zone around the tunnel would increase when the ratio of σ_{cm}/σ_v was less than 0.25, as it was above the case of Meninting tunnel of 0.13.

However, under seismic forces, the stability of the Meninting tunnel was very much influenced by earthquake forces, similar to that for buildings (Kencanawati *et al.*, 2020). The FoS of the tunnel reduced significantly, particularly on the tangential directions of 0^0 on the horizontal line, 45^0 up and down the horizontal line, when earthquake forces worked on horizontal direction. The HB strength criterion seems to have less sensitive to the influence of earthquake forces, rather depends on rock properties. The MMC criterion still provided the FoS above 2.5 under all seismic conditions; although, the proposed seismic parameters by Agustawijaya *et al.* (2020b) provided more

reductions to the stability of the tunnel compared to SNI 1926:2019 and SNI 1926:2019. As the earthquake data for the SNI 1726:2019 were adopted from Irsyam *et al.* (2017), they might not yet represent seismic condition after a series of earthquake events in 2018.

One solution of many suggestions (Hoek and Brown, 1994) would be the improvement of the application of grouting and rock bolting installations (Aldiamar *et al.*, 2015). This could increase the shear strength, leading to reduce deformation of rock masses (Zhang *et al.*, 2016; Agustawijaya *et al.*, 2020a). A rock mass-support system interaction analysis could, therefore, be conducted as by Soenarso (1994) and Harjomuljadi (2010).

The most significant influence for a shallow tunnel is σ_{cm}, which in turn will depend on friction characteristics of the rock (Stiros and Kontogianni, 2009). The failure mechanism of the rock will depend on how shear forces working on the rock, most probably shear forces due to earthquake. But, the stability of a structure at shallow depths could be subjected to ground subsidence caused by gravity loads, thus, in general it will depend very much on rock characteristics, then shear, tension, and compression stresses generated by earthquakes.

The Meninting tunnel construction might be sufficient to stand earthquake stresses, but since it was excavated into a hill of various volcanic rock materials, the stability of rock masses would be a problem. On the top of the tunnel, loose bouldery agglomerates and colluviums would have low strength, particularly with a high coefficient of permeability; they could easily lose their shear strength under earthquake forces. As the events in 2018, the surrounding area of the Miniting dam collapsed, where many landslides occurred during the events (Irsyam *et al.*, 2018). Modeling shows that the upper tunnel cross section could be more vulnerable than the lower part, but it might due to the PGA<0.3 g (Wen *et al.*, 2017). Therefore, the stability of the tunnel would not only depend on the support systems installed to the tunnel, but it also could depend on the stability of residual rock mass strength around the tunnel.

According to Brady and Brown (1993), dynamic shear strength (Equation 4) could drop 10% from static shear strength (Equation 3). Research on the Luk Barat bridge of North Lombok Regency after Lombok earthquake events in 2018 (Agustawijaya *et al.*, 2019) found that residual shear strength of tuffaceous sandstone of the Lekopiko Formation could drop 41% from that before the events when the bridge was designed. Similarly, the strength drop of the same rock formation might occur at the Meninting tunnel. When residual shear strength is considered to be the strength of rock masses around the tunnel, the FoS of the tunnel could be as low as 2.43 using the MMC on the Wall C. Thus, the diversion-spillway tunnel of the Mininting dam might have a stability problem on rock masses around the tunnel due to similar severe earthquakes in the future.

CONCLUSION

The Lombok earthquake 2018 has changed seismic conditions of Lombok Island, and changed seismic parameters for construction. The Meninting dam and its diversion-spillway tunnel were designed according to seismic parameters before the 2018 events; they should therefore face consequences in their construction. Current seismic parameters of peak ground acceleration (PGA), short and long spectrum parameters (Ss and S_1) would reduce the stability of the tunnel by 69% soon after the construction, and stand up time should also reduce from one week to probably 25 minutes. Support systems should be applied immediately; these would result in a factor of safety of the tunnel above 2.5 under the influence of earthquake forces, when the modified Mohr-Coulomb criterion was applied. However, this would not be the case for the application of the Hoek-Brown criterion, since it depends on rock properties and confining pressure. As, the Meninting diversion-spillway tunnel was constructed into volcanic breccias at the surface; it was significantly influenced by shear forces. When such forces were generated by earthquakes,

the tunnel certainly required improvement in its support systems. These could mean a lot of additional grouting and rock bolt installations to reduce shear failures of rock masses around the tunnel.

REFERENCES

Agustawijaya, D.S., 2007. The uniaxial compressive strength of soft rock. *Civil Engineering Dimension*, 9 (1)*,* p.9-14.

Agustawijaya, D.S., 2018. Influence of rock properties in estimating rock strength for shallow underground structures in weak rocks. *Indonesian Journal on Geoscience*, 5 (2), p.93-105.

Agustawijaya, D.S., 2019. Practical applications of strength criteria in civil engineering design for shallow tunnel and underground structures in weak rocks. *International Journal of Technology*, 5 (2), p.93-105.

Agustawijaya, D.S., Karyadi, K., Krisnayanti, B.D., and Sutanto, S., 2017. Rare earth element contents of the Lusi mud: An attempt to identify the environmental origin of the hot mudflow in East Java - Indonesia. *De Gruyter Open Geoscience*, 9, p.689-706.

Agustawijaya, D.S., Meyers, A., and Priest, S.D., 2004. Engineering properties of Coober Pedy rocks. *Australian Geomechanics*, 39 (1)*,* p.19-27.

Agustawijaya, D.S., Sulistiyono, H., and Elhuda, I., 2018. Determination of the seismicity and peak ground acceleration for Lombok Island: An evaluation on tectonic setting. *MATEC Web of Conference*, 195 (03018).

Agustawijaya, D.S., Sulistyowati, T., Layli, B.A., and Agustawijaya, A.R., 2019. The ground deformation of the Luk Barat Bridge afterLombok earthquakes 2018. *IOP Conference Series: Earth and Environmental Science*, 389, 012051. DOI: 10.1088/1755-1315/389/1/012051.

Agustawijaya, D.S., Sulistiyono, H., Wahyudi, M., Yasa, I.W., Ashari, K.F., and Agustawijaya, A.R., 2020a. Grouting performance of the Pandan Duri dam shacked by Lombok earthquake 2018. *MATEC Web of Conference*. 331, 02004. DOI: 10.1051/matecconf/202033102004.

Agustawijaya, D.S., Taruna, R.M., and Agustawijaya, A.R., 2020b. An update to seismic hazard levels and PSHA for Lombok and surrounding islands afterearthquakes in 2018. *Bulletin of the New Zealand Society for Earthquake Engineering*, 53 (4)*,* p.215-226.

Al-Awad, M.N.J., 2012. Evaluation of Mohr-Coulomb failure criterion using unconfined compressive strength. *7th Asian Rock Mechanics Symposium*, Seoul, Korea.

Aldiamar, F., Kartikasari, S., and Desyanti, 2015. *Metode perencanaan penggalian dan sistem perkuatan terowongan jalan pada media campuran tanah-batuan.*PedomanBahan Konstruksi Bangunan Dan Rekayasa Sipil, Kementerian Pekerjaan Umum, 45pp (in Indonesian).

Andi Mangga, S, Atmawinata, S., Hermanto, B., and Setyogroho, B., 1994. *Geological Map of the Lombok Sheet, West Nusa Tenggara, Scale 1:250.000*. Geological Research and Development Centre, Bandung.

BMKG (Indonesian Agency for Meteorology, Climate and Geophysics), 2018. Press Release No: UM.505/3/D3/VIII/2018 (in Indonesia). https://www.facebook.com/InfoBMKG/posts/10156548339904931 [8 October 2018].

BSNI (Badan Standardisasi Nasional), 2012. *SNI 1726:2012 Tata Cara Perencanaan Ketahanan Gempa Untuk Struktur Bangunan Gedung dan Non Gedung*, 138pp (in Indonesian).

BSNI (Badan Standardisasi Nasional), 2019. *SNI 1726:2019 Tata Cara Perencanaan Ketahanan Gempa Untuk Struktur Bangunan Gedung dan Non Gedung*, 238pp (in Indonesian).

BSW (Balai Wilayah Sungai), 2017. *Sertifikasi Disain Bendungan Meninting di Kabupaten Lombok Barat.* Laporan Utama, Satuan Kerja Balai Wilayah Sungai Nusa Tenggara I (in Indonesian).

Bieniawski, Z.T., 1989. *Engineering Rock Mass Classifications*, John Wiley & Sons, New York, 272pp.

Bock, Y., Prawirodirdjo, L., Genrich, J.F., Stevens, C.W., McCaffrey, R., Subarya, C., Puntodewo, S.S.O., and Calais, E., 2003. Crustal motion in Indonesia from global positioning system measurements. *Journal of Geophysical Research*, 108 (B8), 2367. DOI: 10.1029/2001JB000324.

Brady, B.H.G. and Brown, E.T., 1993. *Rock Mechanics for Underground Mining*, 2nd Edition, Chapman and Hall, London, 571pp.

De Farias, M.M., Moraes Jr, A.H., and De Assis, A.P., 2004. Displacement control in tunnels excavated by the NATM:3-D numerical simulations. *Tunnellingand Underground Space Technology*, 19, p.283-293.

Eberhardt, E., 2012. ISRM suggested method: The Hoek-Brown failure criterion. *Rock Mechanics and Rock Engineering*, 45, p.981-988.

Griffin, J. and Davies, G., 2018. *Earthquake Sources of the Australian Plate Margin: Revised Models for the 2018 National Tsunami and Earthquake Hazard Assessments*. Geoscience Australia, Record 2018/31, Canberra. DOI: 10.11636/Record.2018.031 [23 January 2020].

Hamilton, W., 1974. *Earthquake Map of Indonesian Region*. USGS, Folio of the Indonesia Region, Map 1-875-C, Scale 1:5000000.

Hamilton, W., 1979. *Tectonics of the Indonesian Region*. U.S. Geological Survey Professional Paper 1078, 345pp.

Harding, T. and Lowell, J., 1979. Structural styles, their plate-tectonic habitats, and hydrocarbon traps in petroleum provinces. *The American Association of Petroleum Geologists Bulletin*, 63 (7)*, p.1016-1058.

Harjomuljadi, S., 2010. *Terowongan dengan NATM*. Mediatama Saptakarya, Jakarta, 90pp (in Indonesian).

Hoek, E. and Brown, E.T, 1994. *Underground Excavations in Rock*, Chapman & Hall, London, 525pp.

Hoek, E., Carranza-Torres, C. and Corkum, B., 2002. Hoek-Brown failure criterion - 2002 edition, *Proceedings of NARMS-TAC Conference*, Toronto, p.267-273.

International Society for Rock Mechanics (ISRM), 1981. *Rock Characterization, Testing and Monitoring, ISRM Suggested Methods*, Brown, E.T. (ed.), Pergamon Press, Oxford, 280pp.

Irsyam, M., Hanifa, N.R., and Djarwadi, D., 2018. *Kajian Rangkaian Gempa Lombok, Provinsi Nusa Tenggara Barat*. Pusat Studi Gempa, Pusat Litbang Perumahan dan Pemukiman, Kementerian Pekerjaan Umum dan Perumahan Rakyat, Jakarta, 196pp (in Indonesian).

Irsyam, M.,Widiyantoro, S., Natawidjaja, D., Meilano, I., Rudyanto, A., Hidayati, S., Triyoso, W., Hanifa, N., Djarwadi, D., Faizal, L., and Sunarjito, S., 2017. *Peta Sumber dan Bahaya Gempa Indonesia Tahun 2017*, Bandung. Pusat Gempa Nasioal (PUSGEN), Kementerian Pekerjaan Umum dan Perumahan Rakyat, 376pp (in Indonesian).

Katili, J.A., 1989. Evolution of the Southeast Asian Arc Complex. *Geologi Indonesia*: *Journal of the Indonesian Association of Geologist*, 12 (1)*, p.113-143.

Kencanawati, N.N., Agustawijaya, D.S., and Taruna, R.M., 2020. An investigation of building seismic designparameters in Mataram City using Lombok earthquake 2018 ground motion. *Journal of Engineering and Technological Sciences*, 52 (5), p.651-664.

Koulali, A., Susilo, S., McClusky, S., Meilano, I., Cummins, P., Tregoning, P., Lister, G., Efendi J., and Syafi'i M.A., 2016. Crustal strain partitioning and the associated earthquake hazard in the Eastern Sunda-Banda Arc. *Geophysical Research Letters*, 43, p.1943-1949.

Kulhawy, F.H., Phoon, K.K. and Prakoso, W.A., 2001. Uncertainty in basic properties of geomaterials. https://www.researchgate.net/publication/265144821 [20 April 2018].

Labuz, J.F. and Zang, A., 2012. ISRM suggested method: Mohr-Coulomb failure criterion, *Rock Mechanics Rock Engineering*, 45, p.975-979.

Lavigne, F., Degeai, J.P., Komorowski, J.C., Guillet, S., Robert, V., Lahitte, P., and Wassmer, P., 2013. Source of the great AD 1257 mystery eruption unveiled, Samalas volcano, Rinjani volcanic complex, Indonesia. *Proceedings of the National Academy of Science*, 110 (42), p.16742-16747.

Martin, C.D., Kaiser, P.K., and Christiansson, R., 2003. Stress, instability and design of underground excavations.*International Journal of Rock Mechanics and Mining Sciences*. DOI: 10.1016/S1365-1609(03)00110-2.

Martin, C.D., Kaiser, P.K., and McCreath, D.R., 1999. Hoek-Brown parameters for predicting the depth of brittle failure around tunnels.*Canadian Geotechnical Journal*, 36, p.136-151.

Prakoso, W.A. and Kulhawy, F.H., 2011. Effects of testing conditions on intact rock strength and variability. *Geotechnical and Geological Engineering*, 29, p.101-111.

Pramono, S., 2018.*Perencanaan Rekonstruksi Wilayah Lombok Berbasis Mitigasi Gempabumi*. Badan Meteorologi, Klimatologi dan Geofisika, Jakarta (in Indonesian). https://cdn.bmkg.go.id/web/Artikel_20181002115022_u1dpuf_-Perencanaan-Rekontruksi-Wilayah-Lombok-Berbasis-Mitigasi-Gempabumi.pdf#viewer.action=download [22 October 2018].

Pranantyo, I.R. and Cummins, P.R., 2019. Multi-data-type source estimation for the 1992 Flores earthquake and tsunami. *Pure and Applied Geophysics*. 176 (7), p.3969-2983. DOI: 10.1007/s00024-018-2078-4 [23 January 2020].

Priest, S.D., 1993. *Discontinuity Analysis for Rock Engineering*. Chapman & Hall, London, 473pp.

Serra, J.B. and Miranda, L., 2013. Ground uncertainty in the application of the observational method to underground works: Comparative examples, in Foundation Engineering in the face of uncertainty: Honoring Fred H. Kulhawy. Withlam, J.L., Phoon, K.K., Hussein, M. (Eds.), *Special Publication, Geo-Congress*, March 3-7, 2013, San Diego, pp.254-270. DOI: 10.1061/9780784412763.

Soenarso, W.S., 1994. *Implementation of Rock-Support Interaction Theory in Assessing The Stability of Underground Openings*. Masters Thesis, Department of Mining Engineering, University of South Australia Gartrell School of Mining, Metallurgy and Applied Geology, Australia, 240pp.

Stiros, S.C. and Kontogianni, V.A., 2009. Coulomb stress changes: From earthquake to underground excavation failures. *International Journal of Rock Mechanics & Mining Sciences*, 46, p.182-187.

Taruna, R.M., 2019. Masters Thesis, University of Mataram, 82pp (in Indonesian).

USGS (United State Geological Survey), 2018. https://earthquake.usgs.gov/earthquakes/search/ [31 December 2018].

Verstappen, M.T., 2010. Indonesian landforms and plate tectonics. *Indonesian Journal on Geoscience*, 5 (3), p.197-207. DOI: 10.17014/ijog.v5i3.103

Wen, K., Shimada, H., Sasaoka, T., and Zhang, Z., 2017.Numerical study of plastic responseof urban underground rock tunnel subjectedto earthquake. *International Journal of Geo-Engineering*, 8 (28). DOI: 10.1186/s40703-017-0066-7 [2 November 2018].

Zhang, B., Li, S., Xia, K., Yang, X., Zhang, D., Wang, S., and Zhu, J., 2016.Reinforcement of rock mass with cross-flaws using rock bolt. *Tunnelling and Underground Space Technology*, 51, p.346-353.